

## Biological Effects of Field Emission-Type X-Rays Generated by Nanotechnology

Tomoharu NAKAZATO<sup>1</sup>, Makoto NAKANISHI<sup>2</sup>, Shigetomo KITA<sup>3</sup>,  
Fumio OKUYAMA<sup>3</sup>, Yuta SHIBAMOTO<sup>4</sup>  
and Takanobu OTSUKA<sup>1\*</sup>

### Field emission/X-ray/Nanotechnology/Carbon nanotube.

Thermionic emission (TE)-type X-ray generators have been exclusively used in medicine, but there are many difficulties in making these X-ray sources compact. A field emission (FE)-type X-ray generator using carbon nanotubes is a newly-developed compact system that can be as small as several cm in length. Considering the compactness of the equipment, the FE-type X-ray generator may become a useful tool for endoscopic, intracavitary or intraoperative radiotherapy in the future. The aim of this study was to investigate the biological effects of X-rays generated by the FE-type X-ray source in comparison with those of conventional TE-type X-rays. Mouse thymic lymphoma 3SB cells were irradiated by an FE-type X-ray generator developed by our group and a conventional TE-type X-ray source under identical conditions. DNA damage after radiation was detected by foci formation of phospho-H2AX ( $\gamma$ -H2AX). Effect on the cell cycle was analyzed by flow cytometry. Activation of the DNA damage checkpoint was analyzed by immunoblotting. Induction of apoptosis was studied using the TUNEL assay. In terms of induction of DNA damage (DNA double-strand breaks), activation of cell cycle checkpoints (p53 stabilization, p21 induction, Chk1 and Chk2 phosphorylations), and induction of apoptotic cell death, FE-type X-rays were as effective as TE-type X-rays, and FE-type X-rays appeared to be applicable to radiation therapy.

### INTRODUCTION

For field emission (FE)-type X-ray sources, electrons striking a metal target are generated by a field emitting process, a quantum-mechanical process of electron tunneling (Fig. 1).

FE source has a protruding shape and is frequently (often, typically) made of “carbon nanotubes” (CNTs).<sup>1)</sup> Since electron tunneling critically depends on the chemical state of the electron-emitting surface,<sup>2)</sup> FE is unstable in non-ultrahigh vacuum (non-UHV) ambiances, especially for metallic cathodes that chemically react with gaseous

molecules remaining in a non-UHV (Non-UHV ambience contains a large number of gaseous molecules, mostly H<sub>2</sub>O molecules).

CNTs are helical microtubules of graphitic carbon, ranging from 4 to 30 nm in diameter and up to 1 mm in length.<sup>3)</sup> Chemically, carbon is far more stable than metals, and CNTs were therefore previously predicted to be promising FE sources.<sup>4)</sup> CNTs have recently been confirmed to field-emit electrons for a long period in X-ray tubes pumped down to a non-UHV.<sup>5–8)</sup>

Since FE requires no cathode heating, the entire tube structure of the FE-type X-ray generator could be miniaturized to be as small as several cm in length. Such a miniature X-ray tube,<sup>9)</sup> which is absolutely unattainable with conventional thermionic emission (TE)-type X-ray tubes,<sup>10)</sup> may play a role in clinical radiation therapy for the purpose of targeted X-ray irradiation to a superficial lesion. Since the FE-type X-ray source has been developed only recently by the group of Okuyama *et al.*,<sup>1)</sup> biological effects of the X-ray have not yet been investigated. Moreover, some differences have been proven to exist between FE- and TE-type X-rays with respect to energy spectra. Therefore, it is necessary to investigate whether biological effects of FE type X-rays are similar to those of TE type X-rays before consider-

\*Corresponding author: Phone: +81-52-853-8236,

Fax: +81-52-842-0266,

E-mail: t.otsuka@med.nagoya-cu.ac.jp

<sup>1)</sup>Department of Musculoskeletal Medicine; <sup>2)</sup>Department of Biochemistry and Cell Biology and <sup>4)</sup>Department of Radiology, Nagoya City University, Graduate School of Medical Sciences, 1 Kawasumi, Mizuho-cho, Mizuho-ku, Nagoya 467-8601, Japan; <sup>3)</sup>Graduate School of Engineering, Nagoya Institute of Technology, Gokiso-cho, Showa-ku, Nagoya 466-8555, Japan. Abbreviations. FE: Field emission. TE: Thermionic emission. CNT: Carbon nanotube

doi:10.1269/jrr.06071

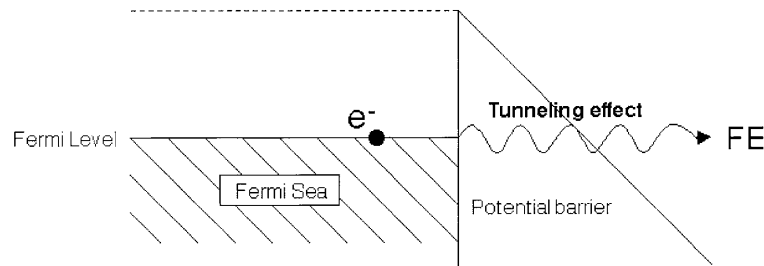


**Fig. 1.** Principle of FE (schematic). Electrons at the Fermi level penetrate the surface potential barrier that becomes thinner under a strong electric field.

ing their application in medicine.

X-ray is a representative agent causing DNA double-strand breaks (DSBs) of cells. Among the many types of damage, DSBs are the most deleterious to cell survival. To maintain genomic integrity, eukaryotic cells are equipped with coordinated systems to contend with DNA damage, including chromatin remodeling, cell cycle arrest, DNA repair and programmed cell death processes.<sup>11–13</sup> Numerous key players, including p53, p21, Chk1 and Chk2, have been identified, and their cooperation in damage control has only recently become evident. Therefore, it appeared meaningful to investigate the biological effects of FE-type X-rays using these endpoints.

In this paper, we present indisputable evidence that FE-type X-rays being emitted from a tungsten target damage DNA, activate cell cycle checkpoints and induce apoptosis in cancer cells cultivated *in vitro*.

## MATERIALS AND METHODS

### Cell culture

The mouse thymic lymphoma cell line 3SB was a gift from the National Institute of Radiological Sciences (Chiba, Japan).<sup>14,15</sup> The cells were maintained in RPMI 1640 medium (Sigma-Aldrich Inc., St. Louis, MO, USA) supplemented with 10% fetal bovine serum, penicillin (100 units/ml), streptomycin (100 mg/ml), and 10 mM HEPES Buffer Solution (Invitrogen Co., Grand Island, NY) at 37°C in a humidified 95% air-5% CO<sub>2</sub> atmosphere. The doubling time of 3SB cells was about 18 h *in vitro*. The cells were seeded at a density of 8–10 × 10<sup>5</sup> cells in 9.6 cm<sup>2</sup> plastic tissue culture dishes with 1.7 ml medium.

### Treatment of the cells with nocodazole

The cells were synchronized at M phase with nocodazole at a concentration of 0.5 mg/ml for 8 h in an incubator and then incubated in a fresh medium for 3 h and irradiated (conditions determined by the results of a preliminary experiment). After these treatments, incubation was continued again.

### Irradiation

The FE-type X-ray system was developed by the group of Okuyama *et al.* at Nagoya Institute of Technology (Nagoya, Japan). It is a slightly modified version of the X-ray system used in a previous study.<sup>8,16</sup> The conventional TE-type X-ray equipment was YXLON MG 226/2.25 (YXLON Int., Tokyo), and the X-ray tube was MCN 225 (Philips Industrial, Hamburg). It has been used for biological studies.<sup>17,18</sup> Characteristics of the two systems are summarized in Table 1.

**Table 1.** Characteristics of the field emission (FE)-type and thermionic emission (TE)-type X-ray sources.

Characteristic	FE-type	TE-type
Tube voltage (kV)	50	50
Current (mA)	1	1
Target	Tungsten	Tungsten
Window	Beryllium	Beryllium
Filter	None	None
X-ray spectra	Characteristic X-rays	Continuous
Source-to-object distance (cm)	12.5	18
Dose rate (Gy/min)	3.3 Gy/min	3 Gy/min
Dose inhomogeneity within samples	< 10%	< 3%

The X-ray spectra of the FE-type equipment obtained with Xflash Spectrometer (Röntec, Berlin, Germany) are shown in Fig. 2. As shown in the figure, the FE-type equipment generates characteristic X-rays almost exclusively, while conventional TE-type equipment with a tungsten target has been reported to generate continuous spectra with almost no peak of characteristic X-rays.<sup>19</sup>

Since the X-ray tube voltage of the FE-type system was 50 kV at maximum, both the FE-type and conventional TE-type sources were operated at 50 kV. Radiation doses were calibrated using a RAMTEC 1500B dosimeter (Toyo Medic, Tokyo, Japan) and a soft X-ray chamber (N 23344-0939, PTW-Freiburg, Germany). Fig. 3 shows the dose distribution

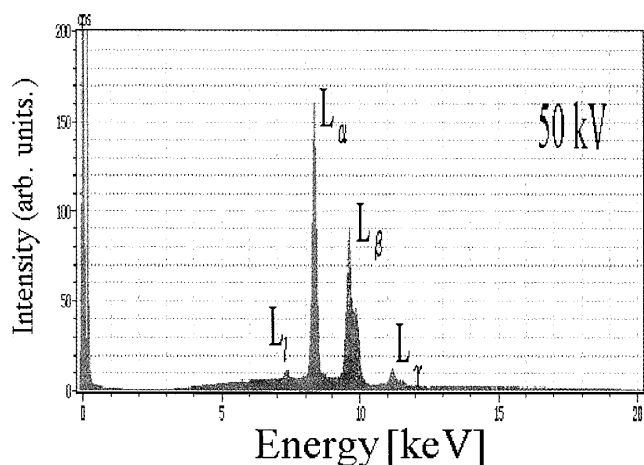


Fig. 2. Spectra of X-rays generated by the FE-type source.

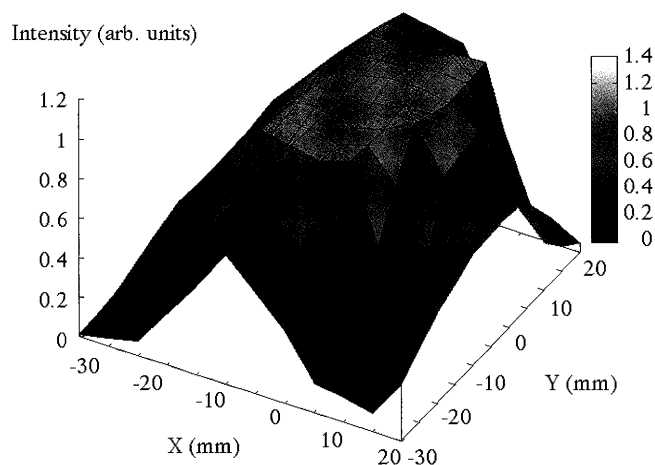


Fig. 3. Dose distribution of the FE-type X-ray (50 kV).

and homogeneity of the FE-type X-rays within the radiation field; in this experiment, culture dishes with an area of 9.6 cm<sup>2</sup> were used and dose inhomogeneity was therefore considered to be less than 10%. The lid of the culture dish was taken off during irradiation.

#### Immunofluorescence microscopy

After 1 h of 3 Gy irradiation, cells were harvested, washed twice in PBS, and fixed in 70% ethanol overnight at -20°C. After the cells had been washed and suspended in PBS at a concentration of  $5 \times 10^4$ /ml, cells in 500  $\mu$ l PBS were attached to micro slide glasses using cytospin and the slide glasses were soaked in PBS. The soaked slides were permeabilized with PBS containing 0.2% Triton X-100 for 5 min and washed twice in PBS. Then they were blocked with 0.05% Tween 20 in 3% skim milk in PBS at room temperature for 1 h and rinsed in PBS. The slides were incubated at room temperature for 2 h with mouse monoclonal anti- $\gamma$ -H2AX (Upstate Cell Signaling Solutions, Lake Placid, NY, 1:100) and for 1 h with Alexa Fluor® 488 goat anti-mouse

IgG (H + L) (Molecular Probes Eugen, Oregon, USA, 1:1000). Finally, the cells were counterstained with 0.1  $\mu$ g/ml 4'-6-Diamidino-2-phenylindole (DAPI) and analyzed using a fluorescence microscope, Nikon Eclipse E800 (Nikon Co., Kanagawa, Japan). Images were captured using a 100  $\times$  oil lens.

#### TUNEL assay

Nuclear DNA fragmentation of apoptotic cells was measured by the TUNEL assay (DeadEnd Fluorometric TUNEL System, Promega, Madison, WI). Briefly, irradiated cells were harvested, washed once in PBS, and resuspended in PBS at a concentration of approximately  $5 \times 10^4$  /ml. Then cells in 500  $\mu$ l PBS were attached to glass slides using cytospin, fixed in 4% formaldehyde, permeabilized in 0.2% Triton X-100, and incubated with TdT incubation buffer for 60 min in a 37°C humidified incubator for 3'-OH labeling. The cells were counterstained with 0.1  $\mu$ g/ml DAPI and analyzed using a fluorescence microscope, Nikon Eclipse E800M at 40  $\times$ . More than 200 cells per coded slide per time were scored for TUNEL labeling.

#### Flow cytometry

After radiation, cells were harvested, washed with PBS, and fixed in 70% ethanol over 4 h. They were counterstained with 50  $\mu$ g/ml propidium iodide (PI) in PBS and analyzed using a flow cytometer and Cell Quest software (Beckton Dickinson Bioscience, San Jose, CA, USA).

#### Immunoblotting and antibodies

Irradiated cells were dissolved in solubilizing buffer (pH 8.0, 50 mM HEPES, 150 mM NaCl, 2.5 mM EGTA, 1 mM EDTA, 1 mM DTT, 0.1% Tween 20, 10% glycerol, and 5 mg/ml phosphatase substrate (Sigma 104®) with the addition of 1 mM sodium fluoride, 0.1 mM sodium orthovanadate and protease inhibitors such as 20  $\mu$ g/ml soybean trypsin, 2  $\mu$ g/ml aprotinin, 100  $\mu$ g/ml PMSF, and 5  $\mu$ g/ml leupeptin. Twenty  $\mu$ g of soluble proteins were separated by 10% sodium dodecyl sulfate-polyacrylamide gel electrophoresis. Separated polypeptides were then transblotted onto a PVDF membrane (Immobilin-P Transfer Membrane, Millipore Co., Billerica, Massachusetts) in transfer buffer (25 mM Tris base, 192 mM glycine, 25 mM sodium dodecyl sulfate, 10% methanol) at 100 V for 30 min at 4°C. Blots were then blocked with 5% skim milk in PBS/0.05% Tween 20 and incubated with the primary antibody at 1  $\mu$ g/ml in 5% skim milk in PBS containing 0.05% Tween 20 for 1 h at room temperature. The secondary antibody was horseradish peroxidase-linked whole antibody, ECL<sup>TM</sup> anti-mouse immunoglobulin G or ECL<sup>TM</sup> anti-rabbit immunoglobulin G (Amersham Biosciences UK, Li., England) at 1:1000 in PBS/0.05% Tween 20. Signals were developed by ECL plus (Amersham Biosciences). Mouse monoclonal antibodies to p53 (Novocastra Laboratories Ltd., Newcastle

upon Tyne, UK) and to p21 (Santa Cruz Biotech, Inc., Santa Cruz, CA) and rabbit polyclonal antibodies to Chk2 (Santa Cruz Biotech.) and to Chk1 phosphorylated on Ser345 and on Ser317 (Cell Signaling Technology, Inc., Danvers, MA) were used. Equal sample loading was confirmed by reprob- ing the sample blots with mouse monoclonal antiserum against  $\beta$ -actin at 0.2  $\mu$ g/ml (Abcam Inc., Cambridge, MA, USA), and the signal was developed by ECL<sup>TM</sup> (Amersham Biosciences).

## RESULTS AND DISCUSSION

### *FE-type X-ray causes DNA damage as efficiently as TE-type X-ray does*

H2AX is known to be a biological marker of DSBs caused by radiation and genotoxic reagents. To examine whether DSBs are actually induced by FE-type and TE-type Xrays, mouse thymic lymphoma 3SB cells were irradiated with FE-

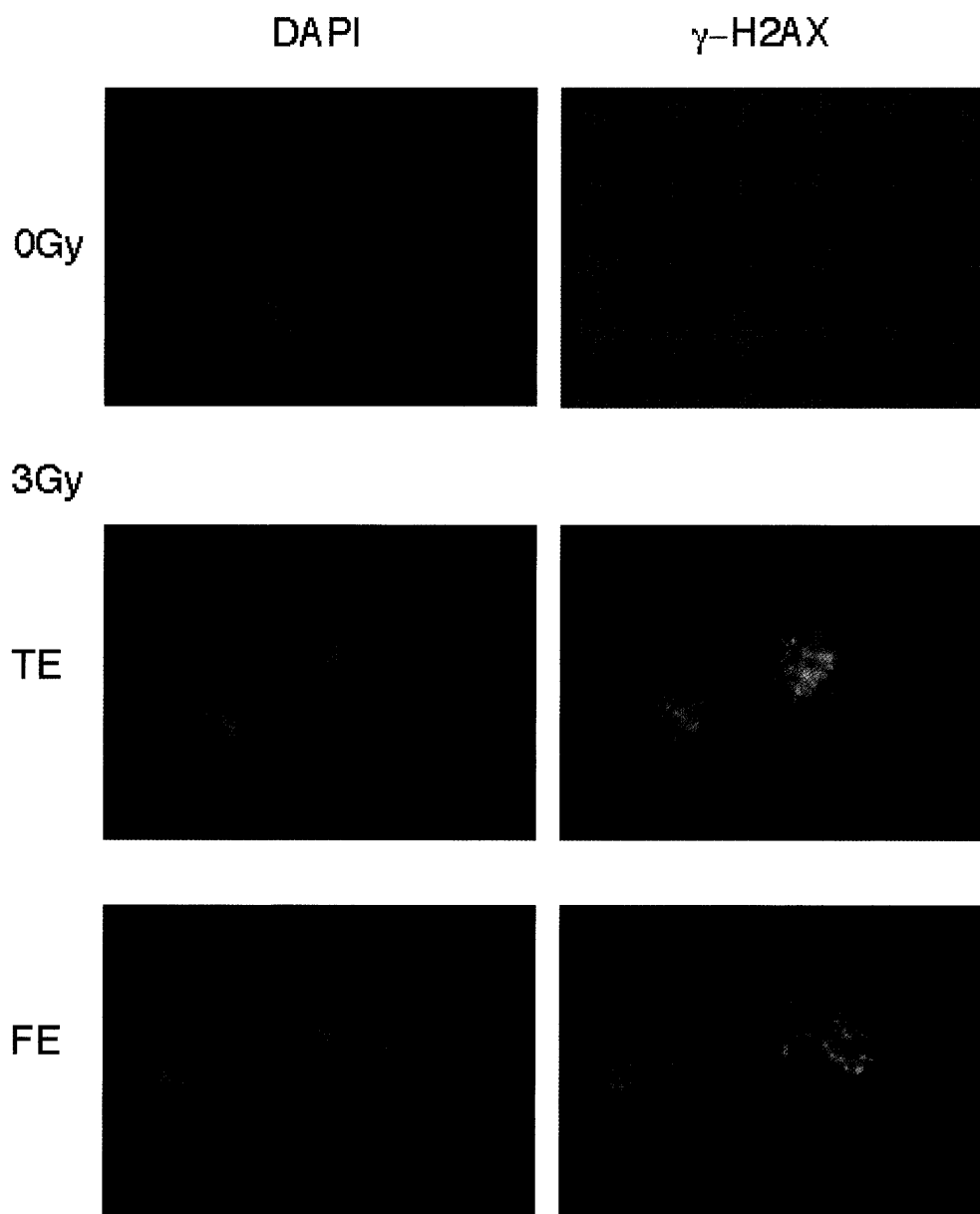


**Fig. 4.** DNA damage after radiation. One h prior to harvest, 3SB cells were treated with ionizing radiation. They were labeled with an anti- $\gamma$ -H2AX antibody and then incubated with a secondary antibody and counterstained with DAPI. The labeled cells were imaged with a confocal microscope at 100 $\times$ . X-ray type and dose are indicated on the left. DAPI staining and  $\gamma$ -H2AX staining are indicated at the top. Both TE and FE showed foci formation of  $\gamma$ -H2AX. Shown are representative micrographs of experiments carried out twice.

type or TE-type X-rays and the resultant DSBs were analyzed by foci formation of phospho-H2AX ( $\gamma$ -H2AX) using an antibody specific to  $\gamma$ -H2AX.<sup>20,21)</sup> As shown in Fig. 4, foci formation of  $\gamma$ -H2AX was evident as early as 1 h after irradiation of FE-type X-rays (3 Gy), and the number of  $\gamma$ -H2AX foci in cells treated with FE-type X-rays was almost the same as that in cells treated with TE-type X-rays. Similar results were also obtained when cells were irradiated with 1 or 5 Gy (data not shown). Thus, these results indicated that FE-type X-rays are as effective as TE-type X-rays in terms of induction of DNA damage.

#### *FE-type X-ray effectively activates the DNA damage checkpoint*

We next determined the extent of DNA damage caused by FE-type or TE-type X-rays by examining cell cycle check-

point activation because it is a highly sensitive assay for evaluation of the extent of DNA damage. The cell cycle of mouse lymphoma 3SB cells was arrested at G2/M phase but not at G1 phase when the cells were irradiated with either TE- or FE-type X-rays (data not shown). G2/M phase arrest by DNA damage is known to be regulated by checkpoint kinases, Chk1 and Chk2, in a PI3KK-dependent manner.<sup>22-28)</sup> Therefore, we examined changes in the modification and the amount of proteins involved in G2/M arrest in response to DNA damage. Although cell cycle arrest at G1 phase was not evident upon DNA damage, the amount of p53 protein<sup>29,30)</sup> was significantly increased and peaked at 3 h after irradiation of FE-type X-rays (Fig. 5a). The amount of p21 Cdk inhibitor protein, which is one of the p53 targets, was also increased, although it was a later event than p53 induction. The magnitudes of increase in amounts of p53

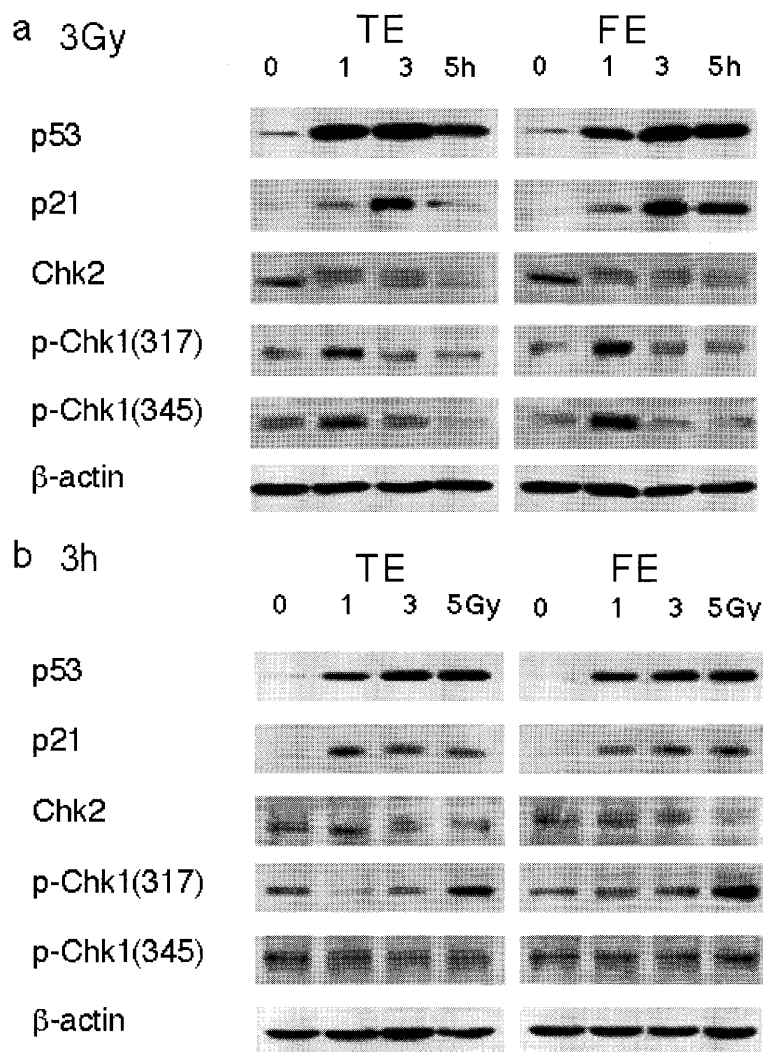


**Fig. 5.** Activation of DNA damage checkpoint after radiation. 3SB cells were exposed to TE- or FE-type X-rays at (a) 3 Gy or (b) indicated doses and harvested at (a) indicated times or (b) 3 h later. Cell lysates were subjected to immunoblot analysis with antibodies specific to p53, p21, Chk2, p-Chk1(317), p-Chk1(345) or,  $\beta$ -actin as indicated.

and p21 caused by FE-type X-rays were almost the same as those caused by TE-type X-rays.

Mobility shift of Chk2 bands<sup>31)</sup> due to phosphorylation was also evident as early as 1 h and continued until 5 h after irradiation. Phosphorylation of Chk1 was also examined using antibodies specific to phospho-Chk1 at Ser317 and phospho-Chk1 at Ser345. As shown in Fig. 5a, Chk1 was abruptly phosphorylated at both Ser317 and Ser345 at 1 h after irradiation and was then dephosphorylated. Importantly, the levels of phosphorylation of Chk2 and Chk1 in cells irradiated with FE-type X-rays were almost the same as those in cells irradiated with TE-type X-rays.

Furthermore, we examined the dose-dependency for modifications of checkpoint proteins by FE- and TE-type X-rays (Fig. 5b). Mouse 3SB cells were treated with the indicated dose of X-rays and then harvested at 3 h. Clear dose-dependent increases in the amounts of p53 and p21 proteins were observed in both cells irradiated with FE-type X-rays and cells irradiated with TE-type X-rays. Phosphorylations of Chk2 and Chk1 were also detected upon treatment with FE- and TE-type X-rays in a dose-dependent manner. Taken together, the results suggest that FE-type X-rays are capable of activating the DNA damage checkpoint as effectively as TE-type X-rays.

#### *Induction of apoptosis by FE-type X ray is independent of cell cycle phase*

The TUNEL assay is a useful tool for the identification of programmed cell death and this method enables a quantification of the process in cell populations. By using this assay, we examined whether irradiation of FE-type X rays indeed induced apoptotic cell death<sup>32)</sup>. As shown in Fig. 6, a time-dependent increase in the number of TUNEL-positive cells was detected in 3SB cells treated with either FE-type or TE-type X-rays. TUNEL-positive cells were first detected as early as 1 h after 1 Gy irradiation ( $13.9 \pm 0.6\%$  with TE and  $9.6 \pm 0.6\%$  with FE) and increased until 5 h ( $25.4 \pm 2.7\%$  with TE and  $27.4 \pm 2.2\%$  in FE). Similar results were also obtained when cells were irradiated with 3 and 5 Gy. These results indicated that irradiation with FE-type X-rays induced apoptotic cell death in time- and dose-dependent manners and that the efficiency of FE-type X-rays for inducing apoptotic cell death was almost the same as that of TE-type X-rays.

Given that certain types of apoptotic cell death are known to be dependent on cell cycle progression,<sup>33)</sup> we also examined whether this is also the case with FE-type X-rays. We synchronized the cell cycle at M phase by nocodazole treatment and then released cells into the cell cycle. Flow cytometric analysis revealed that cells entered S phase at 4 h and entered G2/M phase at 9 h after releasing.

As shown in Fig. 7, the population of subG1-phase cells significantly increased at 4 h and reached a maximum at 6 h after releasing. The increase in the population of subG1-

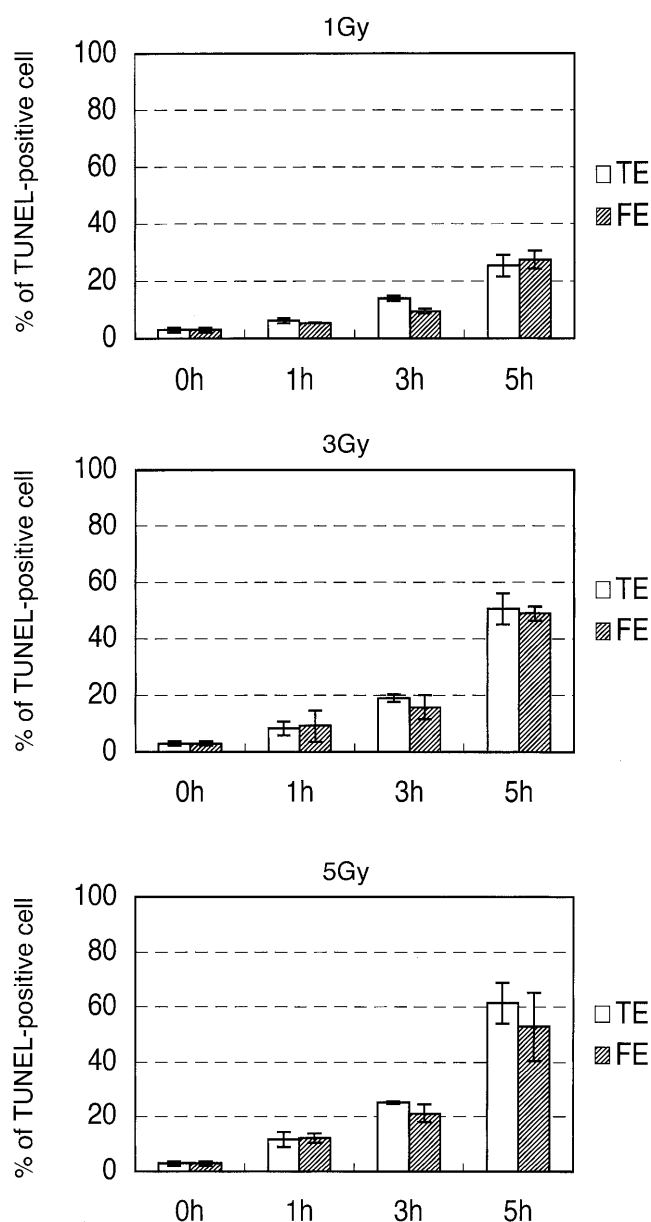


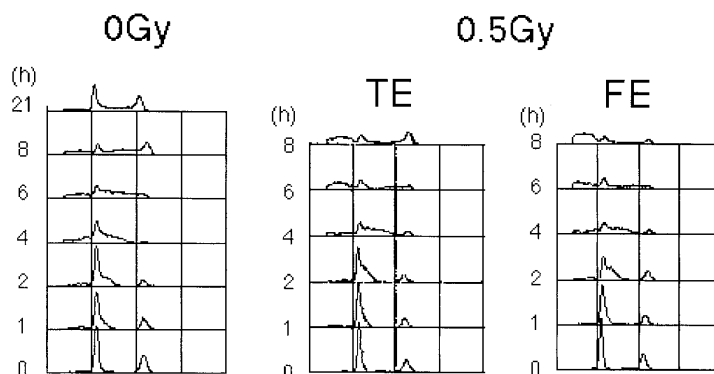
**Fig. 6.** Induction of apoptosis by radiation. (a) Cells were treated with TE-type (open bars) or FE-type (stippled bars) X-rays (indicated doses) and harvested at the indicated times thereafter. They were subjected to TUNEL analysis. The mean values of percentage of TUNEL-positive cells from two independent experiments are presented with error bars.

phase cells upon treatment with FE-type X-rays was similar to that upon treatment with TE-type X-rays. Therefore, these results suggested that the induction of apoptosis by FE- and TE-type X-rays is at least in part dependent on S phase entry.

#### *New type of radiation therapy may be developed in the future*

This study has shown that FE-type X-rays from tungsten

## a Synchronous



## b

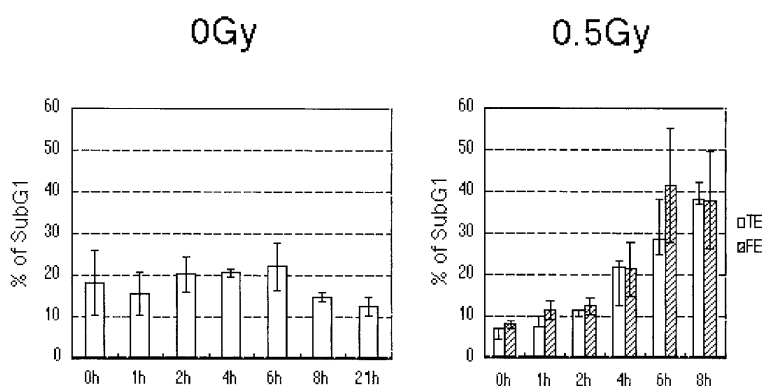


**Fig. 7.** Effect of X-rays on the cell cycle. (a) Representative histograms of synchronous 3SB cells exposed to TE- or FE-type X-rays (0, 0.5 Gy). Cells were treated with nocodazole. Cell cycle analysis was performed for cells harvested at the indicated times thereafter. (b) Cells were treated with nocodazole (upper panel) or in combination with exposure to TE-type (open bars) or FE-type (stippled bars) X-rays (0.5 Gy) (lower panel). The mean values of percentage of Sub G1 from two independent experiments are presented with error bars.

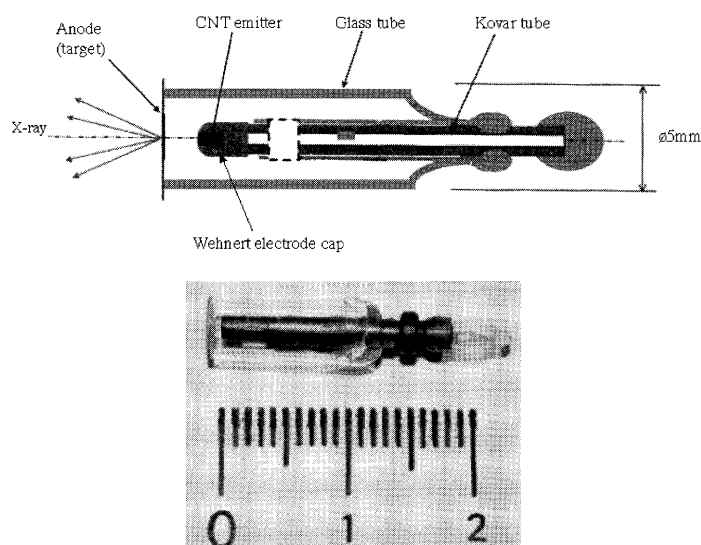


**Fig. 8.** A trial product of the miniature X-ray tube experimentally produced by Okuyama *et al.*<sup>34)</sup> (reproduced with permission).

efficiently cause DNA damage and induce apoptosis in cancer cells. Hence, the FE-type X-ray generator may be applicable to cancer therapy. The entire tube structure of the FE-type X-ray source could be miniaturized as shown in Fig. 8. By coupling with an endoscope and narrowing the radiation field, such a miniature X-ray tube would pave the way to targeted X-ray irradiation of a tumor in the early stage or a superficial lesion and hence may lead to a new strategy for radiation therapy. Although the X-ray tube voltage (50 kV) is lower than conventionally used levels, the issue is practically insignificant and dose inhomogeneity (as shown in Fig. 3) may not be a problem in view of the smallness of lesions that are indicated for such treatment.

### ACKNOWLEDGMENTS

We are grateful to Mr. Hiroyuki Niida and Mrs. Yuko Katsuno for technical assistance and to Mr. Masahiro Muto for preparing the 3SB cell line. This work was supported by 2004 Grants-in-Aid for Scientific Research awarded.

### REFERENCES

1. Sugie, H., Tanemura, M., Filip, K., Iwata, K., Takahashi, K. and Okuyama, F. (2001) Carbon nanotubes as electron source in an X-ray tube. *Appl. Phys. Lett.* **78**: 2578–2580.
2. Fowler, R. H. and Nordheim, L. W. (1928) Electron emission in intense electric fields. *Proc. Roy. Soc. London Ser. A* **119**: 173–181.
3. Iijima, S. (1991) Helical microtubes of graphic carbon. *Nature* **354**: 56–58.
4. Collins, P. G. and Zettl, A. (1997) Unique characteristics of cold cathode carbon-nanotubematrix field emitters. *Phys. Rev.* **55**: 9391–9399.
5. Yue, G. Z., Qiu, Q., Gao, B., Cheng, Y., Zhang, Z., Shimada, H., Chang, S., Lu, J. P. and Zhou, O. (2002) Generation of continuous and pulsed diagnostic imaging of X-radiation using a carbon-nanotube-based field emission cathode. *Appl. Phys. Lett.* **81**: 355–357.
6. Matsumoto, T. and Mimura, H. (2003) Point X-ray source using graphite nanofibers and its application to X-ray radiography. *Appl. Phys. Lett.* **82**: 1637–1639.
7. Yamaguchi, A., Kobayashi, N., Aoki, N., Motoi, Y. and Mitsuoka, Y. (2004) Compact soft X-ray source for biological applications. *Nucl. Sci. Symp.* **N36**: 124–127.
8. Kita, S., Sakai, Y., Fukushima, T., Mizuta, Y., Ogawa, A., Senda, S. and Okuyama, F. (2004) Characterization of field-electron emission from carbon nanofibers grown on Pd wire. *Appl. Phys. Lett.* **85**: 4478–4480.
9. Haga, A., Senda, S., Sakai, Y., Mizuta, Y., Kita, S. and Okuyama, F. (2004) A miniature X-ray tube. *Appl. Phys. Lett.* **84**: 5679–5681.
10. Endo, S., Hoshi, M., Takada, J., Takatsuji, T., Ejima, Y., Saigusa, S., Tachibana, A., Sasaki, M. S. (2006) Development, beam characterization and chromosomal effectiveness of X-rays of RTBC characteristic X-ray generator. *J. Radiat. Res.* **47**: 103–112.
11. Khanna, K. K. and Jackson, S. P. (2001) DNA double-strand breaks: signaling, repair and cancer connection. *Nat. Genet.* **27**: 247–254.
12. Geiman, T. M. and Robertson, K. D. (2002) Chromatin remodeling, histone modifications, and DNA methylation—how does it all fit together? *J. Cell. Biochem.* **87**: 117–125.
13. Vaziri, H., Squire, J. A., Pandita, T. K., Bradley, G., Kuba, R. M., Zhang, H., Gulyas, S., Hill, R. P., Nolan, G. P. and Benchimol, S. (1999) Analysis of genomic integrity and p53-dependent G1 checkpoint in telomerase-induced extended-life-span human fibroblasts. *Mol. Cell. Biol.* **19**: 2373–2379.
14. Ohyama, H., Muto, M. and Yamada, T. (1992) Apoptosis in newly established radiosensitive mouse lymphoma cell lines. Elsevier. Science. Publishers. 361–364.
15. Kawai, H., Yamada, Y., Tatsuka, M., Niwa, O., Yamamoto, K. I. and Suzuki, F. (1999) Down-regulation of nuclear factor  $\kappa$ B is required for p53-dependent apoptosis in X-rayirradiated mouse lymphoma cells and thymocytes. *Cancer Res.* **59**: 6038–6041.
16. Senda, S., Tanemura, M., Sakai, Y., Ichikawa, Y., Kita, S., Otsuka, T., Haga, A. and Okuyama, F. (2004) New field-emission x-ray radiography system. *Rev. Sci. Instrum.* **75**: 1366–1368.
17. Ogino, H., Shibamoto, Y., Sugie, C. and Ito, M. (2005) Biological effects of intermittent radiation in cultured tumor cells: influence of fraction number and dose per fraction. *J. Radiat. Res.* **46**: 401–406.
18. Sugie, C., Shibamoto, Y., Ito, M., Ogino, H., Suzuki, H., Uto, Y., Nagasawa, H. and Hori, H. (2005) Reevaluation of the radiosensitizing effects of sanazole and nimorazole *in vitro* and *in vivo*. *J. Radiat. Res.* **46**: 453–459.
19. Purdy, J. A. (2004) Principles of radiologic physics, dosimetry, and treatment planning. In: *Principles and Practice of Radiation Oncology 4<sup>th</sup> Edition*, Eds. C. A. Perez, L. W. Brady, E. C. Halperin and R. K. Schmidt-Ullrich, pp. 180–218, Lippincott Williams & Wilkins, Philadelphia.
20. Rogakou, E. P., Pilch, D. R., Orr, A. H., Ivanova, V. S. and Bonner, W. M. (1998) DNA double-stranded breaks induce histone H2AX phosphorylation on serine 139. *J. Biol. Chem.* **273**: 5858–5868.
21. Yoshida, K., Yoshida, S. H., Shimoda, C. and Morita, T. (2003) Expression and radiationinduced phosphorylation of histone H2AX in mammalian cells. *J. Radiat. Res.* **44**: 47–51.
22. Rogakou, E. P., Boon, C., Redon, C. and Bonner, W. M. (1999) Megabase chromatin domains involved in DNA double strand breaks *in vivo*. *Cell. Biol.* **146**: 905–915.
23. Gatei, M., Sloper, K., Sørensen, C., Syljuäsen, R., Falck, J., Hobson, K., Savage, K., Lukas, J., Zhou, B. B., Bartek, J. and Khanna, K. K. (2003) Ataxia-telangiectasia-mutated (ATM) and NBS1-dependent phosphorylation of Chk1 on Ser-317 in response to ionizing radiation. *J. Biol. Chem.* **278**: 14806–14811.
24. Zhao, H. and Worms, H. P. (2001) ATR-mediated checkpoint pathways regulate phosphorylation and activation of human Chk1. *Mol. Cell. Biol.* **21**: 4129–4139.
25. Peng, C. Y., Graves, P. R., Thoma, R. S., Wu, Z., Shaw, A. S. and W. H. (1997) P130Cas, Mitotic and G2 checkpoint con-

- trol: regulation of 14-3-3 protein binding by phosphorylation of Cdc25C on serine216. *Science* **277**: 1501–1505.
26. Matsuoka, S., Huang, M. and Elledge, S. J. (1998) Linkage of ATM to cell cycle regulation by the Chk2 protein kinase. *Science* **282**: 1893–1897.
27. Bartek, J., Falck, J. and Lukas, J. (2001) CHK2 kinase—a busy messenger. *Nat. Rev. Mol. Cell. Biol.* **2**: 877–886.
28. Abraham, R. T. (2001) Cell cycle checkpoint signaling through the ATM and ATR kinases. *Genes. & Dev.* **15**: 2177–2196.
29. Jack, M. T., Woo, R. A., Hirao, A., Cheung, A., Mak, T. W. and Lee, P. W. K. (2002) Chk2 is dispensable for p53-mediated G1 arrest but is required for a latent p53-mediated apoptotic response. *PNAS.* **99**: 9825–9829.
30. Levine, A. J. (1977) p53, the cellular gatekeeper for growth and division. *Cell* **88**: 323–331.
31. Gire, V., Roux, P., Thomas, D. W., Brondello, J. M. and Dulic, V. (2004) DNA damage checkpoint kinase Chk2 triggers replicative senescence. *EMBO. J.* **23**: 2554–2563.
32. Gavrieli, Y., Sherman, Y. and Sasson, S. A. B. (1992) Identification of programmed cell death in situ via specific labeling of nuclear DNA fragmentation. *Cell. Biol.* **119**: 493–501.
33. Bernhard, E. J., Maity, A., Muschel, R. J. and Mckenna, W. G. (1995) Effects of ionizing radiation on cell cycle progression. A review. *Radiat. Environ. Biophys.* **34**: 79–83.
34. Senda, S., Sakai, Y., Mizuta, Y., Kita, S. and Okuyama, F. (2004) Super-miniature X-ray tube. *Appl. Phys. Lett.* **85**: 5679–5681.

*Received on August 27, 2006*

*1st Revision received on November 21, 2006*

*2nd Revision received on December 20, 2006*

*Accepted on January 11, 2007*

*J-STAGE Advance Publication Date: February 22, 2007*